arXiv:1405.6861v1 [cond-mat.str-el] 27 May 2014

Nature of itineracy in CoV_2O_4: A first principles study

Ramandeep Kaur, Tulika Maitra* and Tashi Nautiyal

Department of Physics, Indian Institute of Technology Roorkee, Roorkee- 247667, Uttarakhand, India

E-mail: tulimfph@iitr.ac.in (*corresponding author)

Abstract. Inspired by recent experiments, we have theoretically explored the nature of itineracy in CoV_2O_4 under pressure and investigated, using first principles density functional theory calculations, if it has any magnetic and orbital ordering. Our calculations indicate that there could be two possible routes to obtain the experimentally observed pressure induced metallicity in this system. One is the spin-orbit interaction coupled with Coulomb correlation which can take the system from a semiconducting state at ambient pressure to a metallic state under high pressure. The other mechanism, as indicated by our GGA+U calculations, is based on the presence of two types of electrons in the system: localized and itinerant. An effective Falicov-Kimball model could then possibly explain the observed insulator to metal transition. Comparison of the two scenarios with existing experimental observations leads us to believe that the second scenario offers a better explanation for the mechanism of insulator to metal transition in CoV_2O_4 under pressure.

PACS numbers: 71.20.-b, 71.30.+h, 71.70.Ej, 71.27.+a

1. INTRODUCTION

Orbital and magnetic order in spinel vanadates have recently become an intense topic of discussion amongst the experimentalists and theoreticians alike [1]. Several efforts have been made to unravel the complex behavior involving lattice, spin and orbital degrees of freedom of such systems[2]. In spinel vanadates, orbitally active vanadium ions (V^{3+}) at the B-sites of AV_2O_4 form a frustrated pyrochlore lattice. These systems often show multiple structural and magnetic transitions at low temperatures[3, 5, 4]. Things become more interesting when the A-site is also occupied by one of the transition metal (TM) ions which is magnetic. Competing exchange interactions among the spins at A and B sites often result in more than one magnetic transitions with change in temperature and at times in a complicated non- collinear magnetic ordering at low temperatures [4, 6]. Spinel vanadates such as MnV_2O_4, FeV_2O_4 and CoV_2O_4 with magnetic transition metal ions at A and B sites show a ferrimagnetic order of A and B spins at low temperatures where all the vanadium spins are parallel to one another but are antiparallel to those at A sites[7, 8]. Whereas on the other hand, the spinels such as ZnV_2O_4, CdV_2O_4 and MgV_2O_4 having non-magnetic A ion are found to have antiferromagnetically arranged V spins [3, 5]. Usually the latter undergo structural transition followed by a magnetic transition at low temperatures.

From literature it is clear that among the spinel vanadates, CdV_2O_4 resides on the most insulating regime as the vanadium-vanadium distance d_{V-V} in it is the largest. Single crystal measurements [9] reveal that CoV_2O_4 has the shortest d_{V-V} and hence is the closest to the boundary between insulating and metallic regimes. Though this system is semiconducting at ambient pressure, with the application of pressure which reduces d_{V-V} further, it crosses a critical value of d_{V-V} and starts conducting[9]. However, the order of resistivities observed in the pressure induced "metallic" regime is much higher[9] in comparison to the typical resistivities observed in case of a good metal. As far as the transport property is concerned, FeV_2O_4 lies in between CoV_2O_4 and MnV_2O_4. In Table 1 we have summarized the available data from literature for these AV_2O_4 vanadates [3, 4, 5, 7, 9, 10, 11, 12, 13, 14, 15, 16]. We note that as we go from A= Mn to Fe to Co, the d_{V-V} decreases gradually and corresponding magnetic ordering temperature is found to increase. Also, as d_{V-V} approaches the predicted itinerant electron limit ($\sim$2.94 Å) [16], the tetragonal structural distortion decreases approaching the cubic structure.

CoV_2O_4 is a normal spinel having cubic structure with $Fd\bar{3}m$ symmetry where the V ($3d^2$) ions are placed within O_6 octahedra and Co ($3d^7$) ions are placed within O_4 tetrahedra[15]. Crystal field produced by oxygen ions splits the d orbitals in t_{2g} - e_g manifolds. The t_{2g} (e_g) orbitals have lower energy than e_g (t_{2g}) orbitals in octahedral (tetrahedral) field. The O_6 octahedra are not the ideal ones as the O-V-O angles deviate from 90^o in this structure [9, 15]. This distorted octahedron causes a local trigonal distortion which further splits the triply degenerate t_{2g} orbitals of vanadium into an a_{1g} orbital and doubly degenerate e'_g orbitals. In accordance with Hund's rules, V^{3+} in

Table 1. Collected data for various vanadium spinels summarizing the trends. T_S and T_N define the structural and magnetic transition temperatures, respectively. Here AFM, FIM and FM stand for Antiferromagnetic, Ferrimagnetic and Ferromagnetic ordering, respectively.

spinel system	d_{V-V} ($\AA$)	$T_S(K)$	$T_N(K)$	c/a	source
CdV_2O_4	3.072	95	33 (AFM)	0.9877	ref. 9,10,11
MnV_2O_4	3.014	56	56 (FIM)	0.98	ref. 4,7,12
	-	-	53 (non collinear)	-	ref 4,7
FeV_2O_4	2.99	140 (HT)	70 (FIM)	0.988 (HT)	ref. 12,13
		110 (LT)	-	1.016 (LT)	12,13
MgV_2O_4	2.976	65	42 (AFM)	0.9941	ref. 5,14,15
ZnV_2O_4	2.98 (in-plane)	51	40 (AFM)	0.9949	ref. 3,15
	2.97 (off-plane)				ref. 3,15
CoV_2O_4	2.972	-	152(FIM)	1	ref. 9,16
	-	-	59 (non collinear)	-	ref. 16

CoV_2O_4 has spin S=1 with the electrons occupying two out of the three t_{2g} levels.

Many vanadium spinels are observed to undergo two types of transitions as temperature is lowered: first structural (e.g. cubic to tetragonal) and then magnetic (e.g. paramagnetic to anti/ferrimagnetic) (see Table 1). The structural transitions are often accompanied by an orbital order which then drives the magnetic order at low temperatures. However, unlike other vanadium spinels, CoV_2O_4 is reported to have no structural transition as the temperature is lowered [9]. Two magnetic transitions are observed [15] in this system, one at 152 K from paramagnetic to collinear ferrimagnetic ordering between the Co and V spins, and the other at 59 K from collinear ferrimagnetic to non-collinear ferrimagnetic order. Hence CoV_2O_4 makes an interesting study. In view of the experimental observations discussed above, many questions need to be explored theoretically for this compound, like what is the nature of itineracy? The effect of pressure on the electronic structure of this compound, *primarily, the mechanism for insulator to metal transition under pressure*, nature of orbital order (if any), and the role of spin-orbit interaction need to be investigated in detail. We have addressed these issues in the present work using density functional theory (DFT) based calculations.

2. CALCULATIONAL DETAILS

As already stated, CoV_2O_4 has normal cubic spinel structure (with space group $Fd\bar{3}m$ (227)) at all the temperatures. It has two formula units (f.u.) per primitive cell. Co ion is at (3/8,3/8,3/8) which is 8b tetrahedral site, V ion sits at (0,0,0) which is 16c octahedral site, and O ion sits at (x,x,x) which is 32e position. The structural data for calculation are taken from experiment[9], where x=0.239. The structure was then optimized using

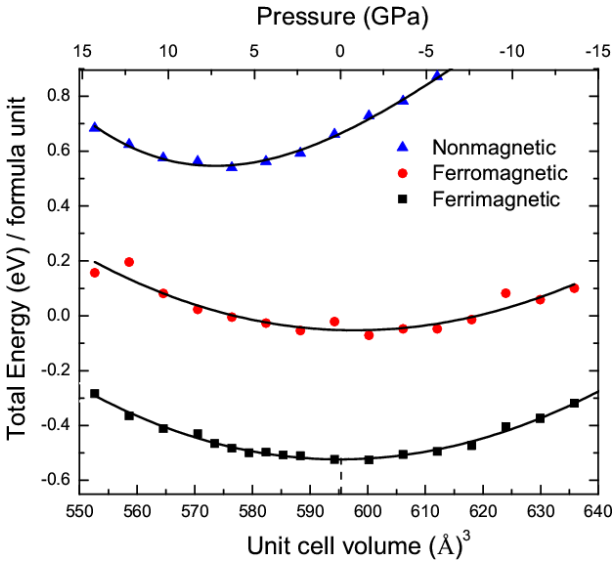

Figure 1. Total Energy vs. conventional unit cell volume of CoV_2O_4 within GGA. Base energy value -97779 eV is to be added to each. The corresponding pressure values are indicated on the top margin. Vertical line marks the equilibrium volume for the energetically favored FIM state.

two different exchange correlation functionals: local spin density approximation (LSDA) and Perdew-Burke-Ernzerhof (PBE) generalized gradient approximation (GGA)[17], within full potential linearized augmented plane wave method as implemented in WIEN2k code[18]. It was observed that the optimized structure obtained within GGA is much closer to the experimental structure than that obtained within LSDA. Hence further calculations were performed using the GGA for exchange correlation. The muffin-tin radii were set to 1.91, 1.94 and 1.69 Å for Co, V and O, respectively. The plane-wave cut off ($R_{mt}.K_{max}$) was set to 8.0, and 72 $\vec{k}$ points were used in the irreducible wedge of the Brillouin zone. The expansion of the radial wave function in spherical harmonics was taken up to angular momentum quantum number $l = 10$. We also performed more refined calculations by including the correlation effects arising from the d electrons of Co and V. For this, we employed self-interaction corrected (SIC) GGA+U approach[19] which takes into account the onsite Coulomb interaction U and removes the self-Coulomb and self-exchange correlation energy. Spin orbit (SO) coupling is included by the second-variational method[20] with scalar-relativistic wave functions. In this approach, firstly the wave functions are calculated for both the spin directions without involving SO interaction term in the eigen value problem. Then those functions are used as basis functions to solve the new eigenvalue problem which has the SO interaction term in the total hamiltonian.

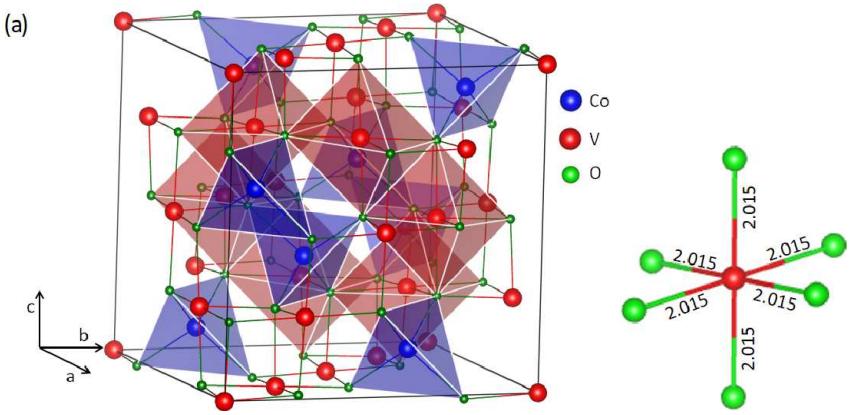

Figure 2. (a) The cubic spinel unit cell for CoV_2O_4. Red (Blue) oxygen octahedra (tetrahedra) are around V (Co) ions. (b) The VO_6 octahedron with bond lengths in Å

3. RESULTS AND DISCUSSION

3.1. Magnetic ordering

Pursuit of a better understanding of the recent experimental observations led us to move to higher levels of sophistication of the calculations: from GGA to GGA+U to GGA+U+SO approximations. In the following, we present the electronic structure calculations within the above approximations and the analysis of the results to propose possible underlying mechanisms to explain the recent experimental findings [9] regarding the effect of pressure on the transport properties of this system. In the process we also studied the effect of pressure on the magnetic and orbital order (if any) of the system. Firstly DFT calculations using GGA were performed to ascertain the magnetic ground state and to obtain the optimized lattice parameters, characterized by the minimum total energy, of CoV_2O_4. Fig. 1 shows the total energy per formula unit as a function of unit cell volume (and of pressure) for Nonmagnetic (NM) or spin unpolarized, Ferrimagnetic (FIM) and Ferromagnetic (FM) arrangements of Co and V spins. We note that for the FIM ordering, Co(V) spins within A(B) sublattice are arranged ferromagnetically, and the two sublattices are ordered antiferromagnetically with respect to each other. It is clearly seen that this material has a strong preference for magnetic states over the NM state since the total energy for the NM state is the highest of all in the studied volume range. It also shows that ferrimagnetic arrangement of Co and V spins constitutes the ground state as the energy of ferromagnetic solution is found to be higher by 0.502 eV/f.u. at the equilibrium volume (= 595.440 $Å^3$). Our calculations predict the equilibrium lattice constant to be 8.4129 Å, larger only by 0.2% compared to the experimental value (8.4073 Å)[9]. We have also calculated the total energy for antiferromagnetic arrangement of vanadium spins as observed in some other spinel vanadates like ZnV_2O_4 and MgV_2O_4[3, 5]. We find that the total energy for such a state at the equilibrium volume is higher than that for the ferrimagnetic case

by 0.181 eV/f.u. Therefore our calculations give FIM ordering as the most favoured one, in agreement with experiments. We have also calculated the equation of state and obtained the bulk modulus and its pressure derivative for the FIM ordering which are found to be 202.23 GPa and 4.09, respectively. These values are comparable to those for other spinel systems [21].

Cation inversion is an interesting phenomenon that is exhibited by some Co spinels such as $CoFe_2O_4$ and $CoAl_2O_4$ [22, 23]. To explore this possibility, we studied the cation inversion in CoV_2O_4 and found that the inverse spinel structure with Co and V at octahedral sites and V at tetrahedral sites has higher energy than the normal spinel structure by 1.126 eV/f.u. This implies that cation inversion is energetically not favoured in CoV_2O_4 as Co and V ions prefer tetrahedral and octahedral sites, respectively. Hence in the following we present our results for the normal spinel structure with optimized unit cell and in the ferrimagnetic ordering.

3.2. GGA calculations

Fig. 2 shows the unit cell for CoV_2O_4 with VO_6 octahedra and CO_4 tetrahedra shaded in different colors. All the Co-O distances and O-Co-O angles have same value equal to 1.981 Å and 109.47^o, respectively. However, the octahedron around V ions is not perfect due to the presence of trigonal distortion. The O-V-O angles deviate by approximately 5^o from the perfect 90^o, having two different values 84.62^o and 95.38^o, though all the V-O distances have same value, equal to 2.015 Å (Fig. 2 (b)). The d_{V-V} distance for the optimized unit cell is 2.974 Å which is fairly close to the limit of itineracy for vanadium spinels predicted from previous studies[16]. In Fig. 3 we present the partial density of states (DOS) for various d states of vanadium within GGA, as well as the total electronic DOS for CoV_2O_4 and of Co, V and O (inset). It clearly shows that the GGA calculations predict a metallic ground state for CoV_2O_4 with a nonzero DOS at the Fermi level (E_F). This is not in agreement with the experimental findings which designate this material as a semiconductor at ambient pressure[9]. It is worth emphasizing that in case of the vanadium ions, a local trigonal distortion is also present, in addition to the octahedral crystal field due to surrounding oxygens. This trigonal distortion further splits the lower energy triply degenerate t_{2g} orbitals into an a_{1g} (d_{z^2}) orbital and the doubly degenerate e'_g orbitals, with the latter having higher energy. We observe from GGA DOS that both a_{1g} (d_{z^2}) and e'_g states are present at the E_F. We note that both Co and V are transition metal ions (having partially filled d orbitals) and are, therefore, expected to be strongly correlated. Hence in order to achieve the experimentally observed semiconducting state, we included the Coulomb correlation in our calculations within GGA+U approximation[19].

3.3. GGA+U: Magnetic, orbital and transport properties

In this section we discuss our results obtained within GGA+U approximation and compare the same with the experimental observations. In an effort to see the impact

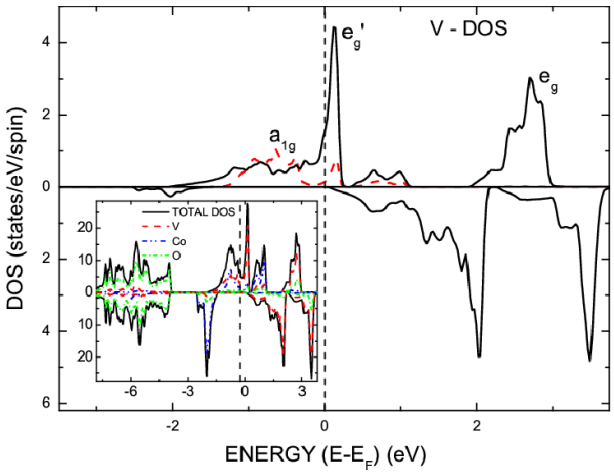

Figure 3. Spin polarized DOS of vanadium within GGA; inset shows the total DOS for CoV_2O_4 and of Co, V and O.

of correlation on the results, we tried various values (ranging from 2 to 5 eV) of U_{eff} (=U-J, where U is the Hubbard parameter representing the on-site Coulomb interaction, and J is the Hund's exchange interaction strength) for both Co and V. Here, we present the results with U_{eff} equal to 4 eV for Co, this also being the usual choice of U_{eff} for Co systems[24]. As discussed in detail below, with this value of U_{eff} for Co, we observe that the occupied Co d states are pushed down far from the E_F leaving mainly the V d states at and around E_F. In Fig. 4 we show the effect of U on the vanadium d states in a range of U_{eff} values which are found relevant also for other vanadium spinels[7, 25]. We discuss later in this section some important physical insights that one can get from Fig. 4 about the possible microscopic mechanism behind the transport properties of this system. We note that the ferrimagnetic arrangement of Co and V spins is found to be the ground state within GGA+U also, with the total energy of this phase being lower than that of the corresponding FM phase by 0.145 eV/f.u.

Fig. 5(a) shows the electronic DOS within GGA+U. The top panel displays the total DOS for Co, V and O; middle and the bottom panels show the DOS for the d states of Co and V, respectively. Tetrahedral crystal field lifts the degeneracy of Co d-orbitals into e_g (i.e. d_{z^2} and $d_{x^2-y^2}$) states with lower energy, and t_{2g} (i.e. d_{xy}, d_{yz}, d_{zx}) states with higher energy. In the majority (down) spin sector, both e_g and t_{2g} orbitals are filled with 5 electrons and the remaining two electrons of Co^{2+} fully occupy the lower lying doubly degenerate e_g orbitals in the minority (up) spin channel. So there are no Co states present at E_F, and with the application of U, the fully occupied d states of Co are further pushed down with respect to E_F.

Comparing our results for V ion with the GGA calculations (discussed in the previous section), we observe that with the application of U, the a_{1g} band is pushed below E_F and with increase in U, goes farther down becoming more and more narrow (localized). On the other hand, the doubly degenerate e'_g bands remain delocalized and

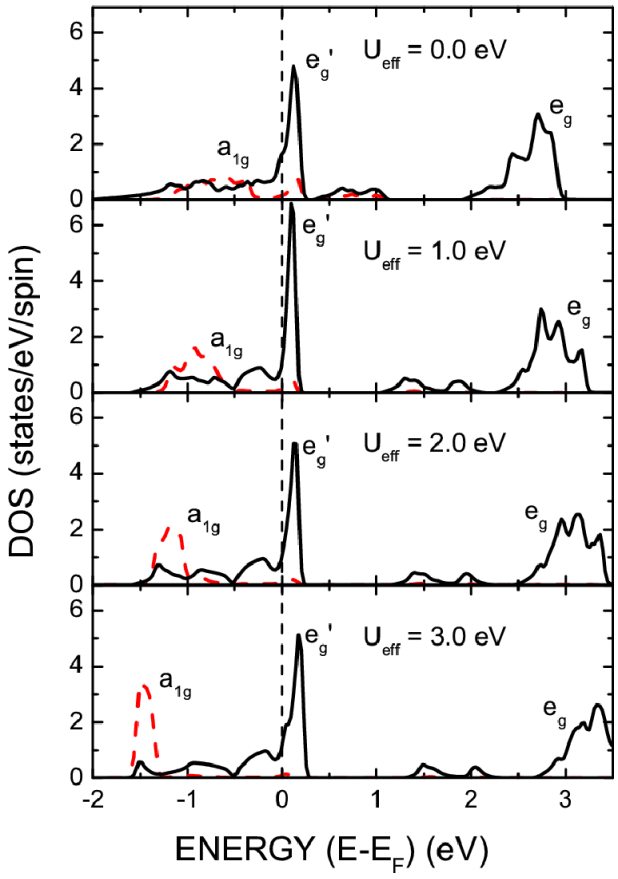

Figure 4. Spin up DOS for vanadium d states around Fermi level within GGA and GGA+U (with U_{eff}=1, 2 and 3 eV) showing increasing localization of a_{1g} states with U.

pinned at the E_F (see Fig. 4). The spin-split a_{1g} band becomes fully occupied by one electron of vanadium. In this case (Fig. 5(a)) with U_{eff} = 2.7 eV[26], the orbital lies well below E_F (by about 1.5 eV). The e'_g bands, which are now seen straddling the E_F, are filled only partially by the 2^{nd} vanadium electron. The system is hence found to be metallic even after taking into account reasonably strong Coulomb correlation in the calculations. However, an important observation one can clearly make from these results is that the system contains two types of electrons: localized and itinerant, as also predicted from a recent experiment[9] on CoV_2O_4 and in accordance with previous theoretical results on similar spinel vanadates[16]. The GGA+U DOS for a_{1g} and e'_g orbitals shown in Fig. 4 strongly suggests that this system can be modelled by a spinless Falicov-Kimball model (FKM) with two degenerate itinerant bands with the Hamiltonian given below

$$H = -\sum_{\langle ij\rangle,\alpha=1,2}(t_{ij}^{\alpha}+\mu\delta_{ij})d_{i\alpha}^{\dagger}d_{j\alpha}+E_f\sum_i(f_i^{\dagger}f_i)+U\sum_{i,\alpha=1,2}(f_i^{\dagger}f_i d_{i\alpha}^{\dagger}d_{i\alpha}) \quad (1)$$

where the a_{1g} state is localized and fully occupied by one electron and the doubly

degenerate e'_g states are itinerant and half filled by one electron[27]. Here $d^\dagger_{i\alpha}, d_{i\alpha}$ are, respectively, the creation and annihilation operators for itinerant e'_g electrons and $f^\dagger_i, f_i$ are the same for localized a_{1g} electrons. $\alpha = 1$ and 2 represent the two degenerate e'_g orbitals. The first term in Eq.(1) is the kinetic energy of e'_g electrons. The second term represents the dispersionless energy level E_f of the a_{1g} electrons while the third term is the on-site Coulomb repulsion between d (or e'_g) and f (or a_{1g}) electrons.

As is well known[28], FKM can give rise to an insulating state (as observed under ambient pressure in CoV_2O_4) due to the strong scattering of the itinerant electrons from the localized ones. The same physics will work even in the presence of two degenerate itinerant bands as long as there is no quantum mixed valence. For infinite dimensions, solutions on FKM [29] reveal that the local inter-orbital susceptibilities, $\chi_{\alpha,f}(\omega)$, diverge with a power law, underlining an incoherent metallic ('bad metal') state. On the application of pressure, the broadening of both itinerant and localized bands would give rise to a small hybridization between the two i.e. the excitonic amplitude such as $< f^\dagger_i d_{i\alpha} >$ then becomes finite (i.e. quantum mixed valence). In that case, it is known that the above model, Equation (1), containing such a hybridizing term can lead to a correlated metal with bad metallic properties[27, 30]. This could be a possible scenario behind the metallic behavior (with high resistivities) under application of pressure. More sophisticated calculations (beyond DFT) such as Dynamical Mean Field Theory (DMFT) [31] could provide useful insight on this mechanism.

3.4. GGA+U+SO: Transport properties under pressure

In an effort to obtain the experimentally observed semiconducting nature of CoV_2O_4 within the limits of DFT, we included the SO coupling in our GGA+U calculations. The SO coupling is known to lift many degeneracies and thus is likely to give rise to the desired gap in the energy spectrum of conduction electrons. Also, it is often found to be significant and has an appreciable effect on the orbital order in other vanadium spinels[13, 25]. In Fig. 5(b) we show the DOS calculated within GGA+U+SO approximation with the same U_{eff} (= 2.7 eV). Magnetization direction is taken to be along (001). What one observes from this DOS is that the complex t_{2g} orbitals are now split into d_1/d_{-1} and d_2. The former has lower energy, lies below the E_F and is occupied with the two vanadium electrons, whereas the latter having higher energy lies above E_F and remains unoccupied. The real d-orbitals are defined in terms of these complex orbitals as $d_{xy} = d_{-2}$-d_2, $d_{xz} = d_{-1}$-d_1, $d_{yz} = d_1$+d_{-1}, $d_{x^2-y^2} = d_2$+d_{-2} and $d_{z^2} = d_0$. It is encouraging to note that this splitting in presence of SO coupling gives the desired gap at the E_F. This energy gap created by SO coupling is about 0.145 eV at ambient pressure which is typical of a semiconductor. More importantly, our results indicate that the inclusion of SO coupling along with the Coulomb correlation is essential to obtain correct ground state of CoV_2O_4 even though it contains only 3-d transition metal elements Co and V. In view of DFT calculations underestimating the band gap, the actual band gap of CoV_2O_4 could be greater than 0.145 eV. There is

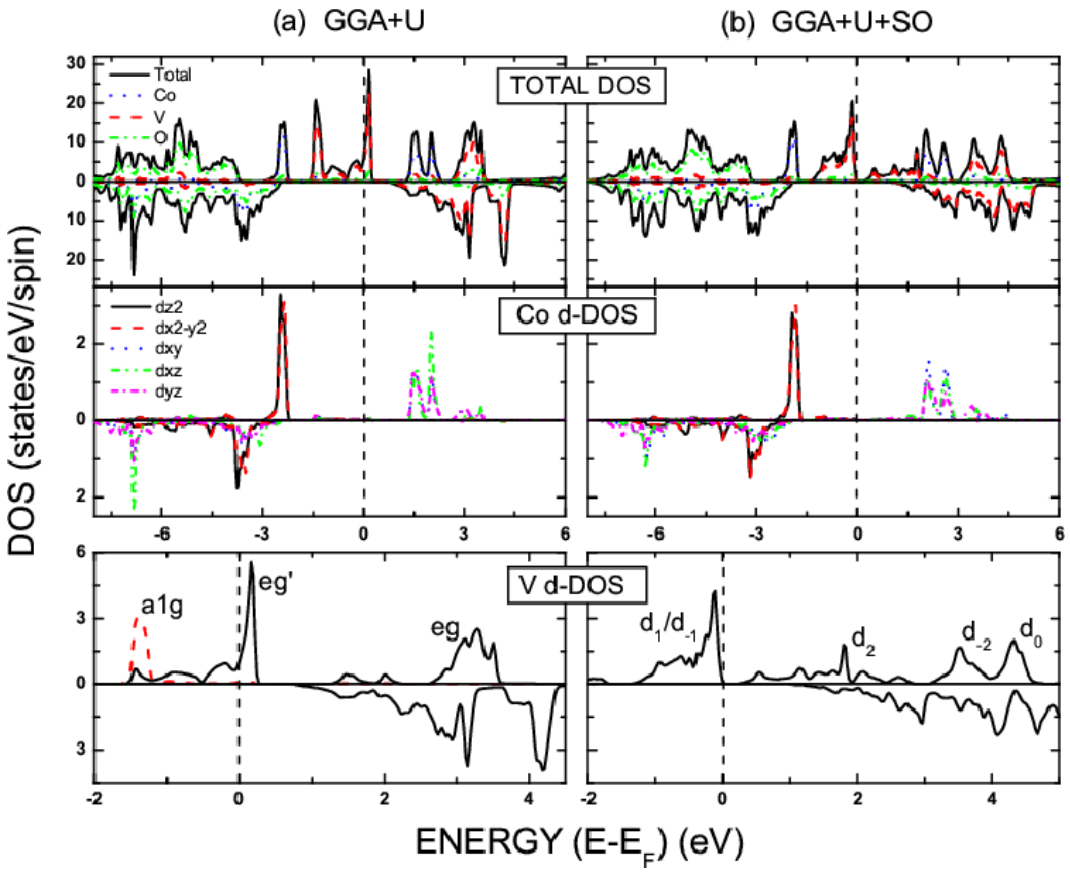

Figure 5. Spin polarized DOS within (a) GGA+U and (b) GGA+U+SO around the Fermi level (U_{eff} = 2.7 eV).

no experimental data available. However, knowing that CoV_2O_4 has d_{V-V} close to the limit of itineracy for these spinel vanadates, we do not expect this band gap to be very large either. It is interesting to note that the d_2 band which lies just above the E_F is very wide (bandwidth about 2.5 eV) compared to the occupied d_1/d_{-1} bands just below E_F (bandwidth about 1 eV).

In recent experiments on CoV_2O_4, Kismarahardja et al. [9] have studied the impact of pressure on the transport properties of this system. They observed that on applying pressure, this system undergoes a semiconductor to metal transition. Though at low temperatures the system remains semiconducting under higher pressures, the metallic character is seen to appear in some intermediate temperature range below T_C where the system has collinear ferrimagnetic order. However, the resistivities observed in the "metallic" phase are an order of magnitude higher than that of typical metals. In fact, the resistivities of the metallic and insulating states are almost comparable in magnitude, only the slopes of resistivity versus temperature have different signs in these two states. The situation is somewhat akin to many of the 'bad metals' found in the literature where the resistivity in the putative metallic state is nearly the same as in the insulating state. This could be a signature of correlated metals (as in other 'bad metals') where strong

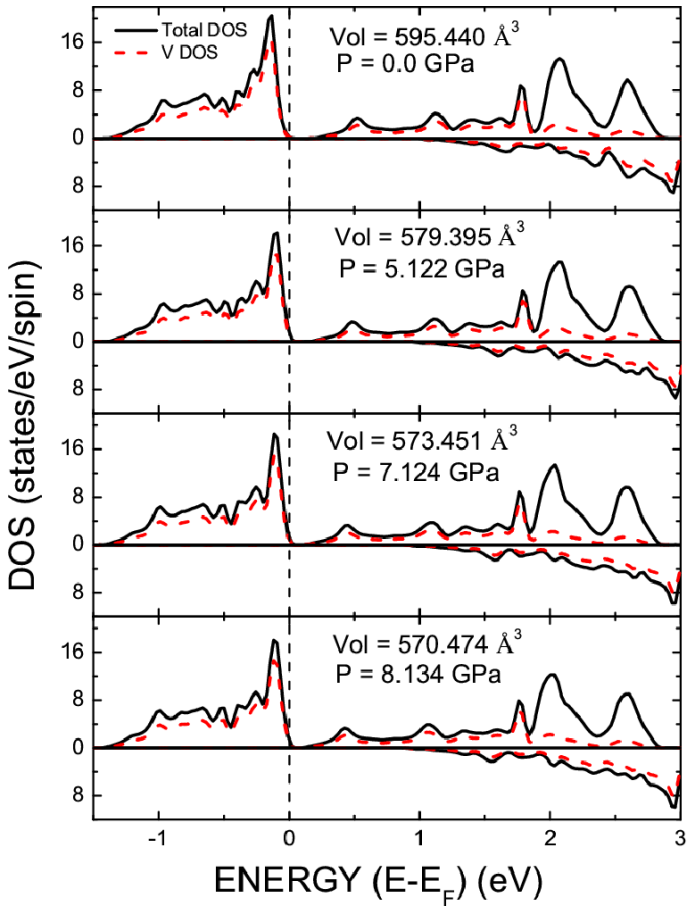

Figure 6. Total DOS and V DOS as a function of energy within GGA+U+SO (U_{eff}=2.7 eV). The pressure (P) and corresponding volume (Vol) values are listed for each panel. The vertical line marks the E_F.

scattering due to electronic correlations dominates the transport. To check if we can recover this transition from our theory, we carried out calculations within GGA+U+SO at different pressures. At this point, we would like to mention that certain cubic spinels such as $ZnGa_2O_4$ [21] are observed to undergo cubic to tetragonal structural transition under pressure. Since no experimental information is available in literature about the distortions introduced by application of pressure on cubic spinel CoV_2O_4, it is worth exploring the possibility of a cubic to tetragonal transition in this system on increasing the pressure. In this context, we performed total energy calculations (within GGA) for the tetragonal structure at 8.134 GPa pressure (close to the highest pressure studied in experiments by Kismarahardja et al.[9]) with both $c/a < 1$ and $c/a > 1$. We observed that both these tetragonal structures have total energy greater than that for the cubic structure with c/a=1. This eliminates the possibility of a cubic to tetragonal structural transition under pressure in CoV_2O_4 in the pressure range studied below. We also note that cubic to tetragonal transition observed by D. Errandonea et al. in $ZnGa_2O_4$ occurs at 31.2 GPa which is much higher than the pressure range studied in this work. Our

interest lies in explaining the experimentally observed change in resistivity in CoV_2O_4 upto 8 GPa, hence we have not explored the higher range of pressure.

The unit cell volumes, all the relevant bond lengths and the corresponding band gaps at various pressures are listed in Table 2. All the bond lengths are seen to decrease with pressure. As the application of pressure in this case does not change the symmetry, the fractional coordinates (x,x,x) of oxygen remain same with increasing pressure. The effect of pressure on the total DOS of CoV_2O_4 is presented in Fig. 6. We can clearly see that with the application of pressure, band gap decreases. It would be interesting to compare this pressure dependence with that of orthovanadates (AVO_4) where such a study was recently reported[32]. Unlike the orthovanadates, we do not see any structural phase transition in the range of pressure studied here. Therefore no discontinuity is observed in band gap versus pressure plot unlike the case of orthovanadates. The calculated pressure coefficient (dE_g/dP) for CoV_2O_4 is found to be about -14.5 meV/GPa. This is comparable to the values measured experimentally in scheelite structures of AVO_4 [32].

As the band gap decreases significantly at higher pressures (for example, at $\simeq$ 8 GPa, the band gap is $\sim$ 27 meV), the system can achieve activated conduction due to thermal excitations across the band gap. As mentioned earlier, the conduction band just above the E_F is highly dispersive compared to the valence band. From the band structure (not shown here) also, we see this feature. So the "metallic" behaviour (with relatively large resistivity) observed in the experiments[9] could be due to the thermal excitations of electrons from the narrow valence band just below the E_F to highly dispersive conduction band just above the E_F. This would, although, essentially be an activated conduction unlike a true metal. The slope of resistivity versus temperature graph will, thus, not change sign unlike that observed experimentally. With further increase in pressure, however, the band gap is expected to close due to the overlap of valence and conduction bands. The system in this case will be highly metallic (even at low temperatures) because of the highly dispersive nature of the conduction band. This is again not consistent with the experimental observations of insulating state at low temperatures and metallic state with high restitivies at intermediate temperatures. So the results presented in this and the previous subsections strongly indicate that the insulator to metal transition observed experimentally in this system under pressure could be better explained through a mechanism involving both itinerant and localized electrons described by Equation (1).

Regarding possible orbital order in this system, we would like to mention that we do not see any orbital ordering as both d_1/d_{-1} orbitals, below the E_F, are degenerate and equally occupied by the two vanadium electrons. Net orbital moment at each vanadium site is also observed to be nearly zero.

Table 2. Variation of unit cell volume, bond lengths (d_{V-V}, d_{Co-O}, d_{V-O}) and band gap with change in pressure using GGA+U+SO

Pressure (GPa)	Volume (Å^3)	d_{V-V} (Å)	d_{Co-O} (Å)	d_{V-O} (Å)	Band Gap (eV)
0.00	595.440	2.974	1.981	2.015	0.145
5.122	579.395	2.947	1.964	1.997	0.085
7.124	573.451	2.942	1.960	1.994	0.053
8.134	570.474	2.932	1.954	1.986	0.0271

4. CONCLUSIONS

Our DFT calculations show that the consideration of Coulomb correlation alone is not enough to obtain the semiconducting nature of CoV_2O_4 at ambient pressure. One has to consider SO interaction in order to reproduce the experimentally observed semiconducting behavior. Our GGA+U+SO results indicate the presence of a highly dispersive conduction band just above the E_F separated from a narrow valence band by a small band gap. With the application of pressure on the system, the band gap is observed to reduce significantly bringing down the wide conduction band very close to the valence band maximum. Therefore, at higher pressures the thermal excitations from the narrow valence band to wide conduction band can lead to an activated conduction. However, the experimental observations that the resistivity of metallic and insulating phases being of the same order clearly indicates that this is a correlated metal rather than simple metal with free electrons. This picture is also borne out in our GGA+U calculations where we do see the presence of two types of electrons: itinerant and localized. So we believe that the insulator to metal transition in this system under pressure can be better explained from an effective spinless Falicov-Kimball model with two degenerate itinerant bands and one localized band as discussed.

5. ACKNOWLEDGEMENT

This work is supported by CSIR, India project grant (ref. no. 03(1212)/12/EMR-II). RK acknowledges CSIR (India) for a research fellowship.

6. REFERENCES

[1] Paolo G Radaelli, New J. Phys. **7**, 53 (2005).
[2] H. Tsunetsugu and Y. Motome, Phys. Rev. B **68** 060405 (2003); *ibid.* Prog. Theor. Phys. Suppl. **160**, 203 (2005).
[3] M. Reehuis, A. Krimmel, N. Bottgen, A. Loidl and A. Prokofiev, Eur. Phys. J. B **35**, 311 (2003).
[4] V. O. Garlea, R. Jin, D. Mandrus, B. Roessli, Q. Huang, M. Miller, A. J. Schultz, and S. E. Nagler, Phys. Rev. Lett. **100**, 066404 (2008).

[5] E.M. Wheeler, B. Lake, A.T. M. Nazmul Islam, M. Reehuis, P. Steffens, T. Guidi and A. H. Hill, Phys. Rev. B **82**, 140406(R) (2010).
[6] J.-H. Chung et al., Phys. Rev. B **77**, 054412 (2008).
[7] S. Sarkar, T. Maitra, Roser Valent, and T. Saha-Dasgupta; Phys. Rev. Lett. **102**, 216405 (2009).
[8] T. Katsufuji, T. Suzuki, H. Takei, M. Shingu, K. Kato, K. Osaka, M. Takata, H. Sagayama, and T. Arima, J. Phys. Soc. Jpn. **77**, 053708 (2008).
[9] A. Kismarahardja, J. S. Brooks, A. Kiswandhi, K. Matsubayashi, R. Yamanaka, Y. Uwatoko, J. Whalen, T. Siegrist, and H. D. Zhou, Phys. Rev. Lett. **106**, 056602 (2011).
[10] G. Giovannetti, A. Stroppa, S. Picozzi, D. Baldomir, V. Pardo, S. Blanco-Canosa, F. Rivadulla, S. Jodlauk, D. Niermann, J. Rohrkamp, T. Lorenz, S. Streltsov, D. I. Khomskii, and J. Hemberger, Phys. Rev. B **83**, 060402(R) (2011).
[11] N. Nishiguchi and M. Onoda, J. Phys.: Condens. Matter **14**, L551 (2002).
[12] A. Kismarahardja, etd-11042010-162636 (2010).
[13] Ramandeep Kaur, T. Maitra and T. Nautiyal, J. Phys.: Condens. Matter **25**, 065503 (2013).
[14] V. Pardo, S. Blanco-Canosa, F. Rivadulla, D. I. Khomskii, D. Baldomir, Hua Wu and J. Rivas, Phys. Rev. Lett. **101**, 256403 (2008).
[15] Y. Huang, Z. Yang and Y. Zhang, J. Phys.: Condens. Matter **24**, 056003 (2012).
[16] S. Blanco-Canosa, F. Rivadulla1, V. Pardo, D. Baldomir, J.-S. Zhou, M. Garca-Hernndez, M. A. Lpez-Quintela, J. Rivas, and J. B. Goodenough,Phys. Rev. Lett. **99**, 187201 (2007).
[17] J.P. Perdew, A. Ruzsinszky, G.I. Csonka, O.A. Vydrov, G.E. Scuseria, L.A. Constantin, X. Zhou, and K. Burke, Phys. Rev. Lett. **100**, 136406 (2008).
[18] P. Blaha, K. Schwartz, G. K. H. Madsen, D. Kvasnicka and J. Luitz, WIEN2K edited by K. Schwarz (Techn. University Wien, Austria, 2001), ISBN 3-9501031-1-2.
[19] V.I. Anisimov, I.V. Solovyev, M.A. Korotin, M.T. Czyzyk, and G.A. Sawatzky, Phys. Rev. B **48**, 16929 (1993).
[20] D.D. Koelling, B N Harmon, J. Phys. C **10**, 3107 (1977); A.H. MacDonald, W E Picket and D D Koelling, ibid. **13**, 2675 (1980).
[21] D. Errandonea, Ravhi S. Kumar, F. J. Manjn, V. V. Ursaki, and E. V. Rusu, Phys. Rev. B **79**, 024103 (2009).
[22] Y H Hou, Y J Zhao, Z W Liu, H Y Yu, X C Zhong, W Q Qiu, D C Zeng and L S Wen, J. Phys. D: Appl. Phys. **43** 445003 (2010).
[23] F. Tielens, M. Calatayud, R. Franco, J. M. Recio, J. Perez-Ramrez and C. Minot, J. Phys. Chem. B, **110**, 988-995 (2006).
[24] Hua Wu, M. W. Haverkort, Z. Hu, D. I. Khomskii, and L. H. Tjeng, Phys. Rev. Lett. **95**, 186401 (2005).
[25] T. Maitra and R. Valentí, Phys. Rev. Lett. **99**, 126401 (2007).
[26] U_{eff}=2.7 eV was chosen in order to ensure that the system remains insulating (consistent with experimental observations) at zero temperature within GGA+U+SO at the highest pressure($\simeq$ 8 GPa) considered in the experiments[9].
[27] U. K. Yadav, T. Maitra, I. Singh and A. Taraphder, Europhysics Letters **93**, 47013 (2011).
[28] L. M. Falicov and J. C. Kimball, Phys. Rev. Lett **22**, 997 (1969).
[29] Q. Si, G. Kotliar, and A. Georges, Phys. Rev. B **46**, 1261 (1992).
[30] A. Taraphder, S. Koley, N. S. Vidhyadhiraja, and M. S. Laad, Phys. Rev. Lett **106**, 236405 (2011).
[31] A. Georges, G. Kotliar, W. Krauth and M. J. Rozenberg, Rev. Mod. Phys. **68**, 13 (1996).
[32] V. Panchal, D. Errandonea, A. Segura, P. Rodriguez-Hernandez, A. Munoz, S. Lopez-Moreno, and M. Bettinelli, Journal of Applied Physics **110**, 043723 (2011).